Bioorganic Chemistry 87 (2019) 720–727

Contents lists available at ScienceDirect

Bioorganic Chemistry

journal homepage: www.elsevier.com/locate/bioorg

Design, synthesis and evaluation of a novel metal chelator as multifunctional agents for the treatment of Alzheimer's disease

Yingying Wang[a], Yue Yang[a], Kwon Ho Hong[b], Yao Ning[a], Ping Yu[a], Jinghui Ren[a], Min Ji[c,d], Jin Cai[a,d,*]

[a] School of Chemistry and Chemical Engineering, Southeast University, Nanjing, Jiangsu 211189, PR China
[b] Department of Medicinal Chemistry and the Institute for Therapeutics Discovery and Development, University of Minnesota, Minneapolis, MN 55414, USA
[c] School of Biological Science & Medical Engineering, Southeast University, Nanjing 210096, PR China
[d] Suzhou Key Laboratory of Biomaterials and Technologies & Collaborative Innovation Center of Suzhou Nano Science and Technology, Suzhou 215123, PR China

ARTICLE INFO

Keywords:
Alzheimer's disease
Multifunctional agents
Acetylcholinesterase inhibitors
Metal chelator
Tacrine
Deferasirox

ABSTRACT

A series of compounds following the lead compounds including deferasirox and tacrine were designed, synthesized and evaluated as multifunctional agents against Alzheimer's disease (AD). In vitro studies showed that most synthesized compounds exhibited good multifunctional activities in inhibiting acetylcholinesterase (bAChE), and chelating metal ions. Especially, compound **TD$_e$** demonstrated significant metal chelating property, a moderate acetylcholinesterase (AChE) inhibitory activity and an antioxidant activity**.** Results from the molecular modeling indicated that **TD** compounds were mixed-type inhibitor, binding simultaneously to the catalytic anionic site (CAS) and the peripheral anionic site (PAS) of *Tc*AChE. Moreover, **TD$_e$** showed a low cytotoxicity but a good protective activity against the injury caused by H_2O_2. These results suggest that **TD** compounds might be considered as attractive multi-target cholinesterase inhibitor and will play important roles in the treatment of AD.

1. Introduction

Alzheimer's disease (AD), first reported in 1906, is rapidly becoming a major threat to healthcare in our society. With more than 48 million people are affected by AD, the number is estimated to show unprecedented growth and increase to spread 131.5 million by 2050 [1,2]. AD is a neurodegenerative disorder clinically characterized with cognitive impairment, the loss of language skills, and ultimately results in complete dependencies and the deaths of the patients with AD [3,4]. Faced with the daunting public health problem of our time, understanding, treatment and prevention of AD are urgent.

Although it has been more than 100 years since AD was first reported, there are many unanswered questions [5]. Due to the etiopathogenesis of AD involving many targets and signaling pathways, various hypotheses have arisen including acetylcholine hypothesis, amyloid deposition hypothesis, oxidative stress hypothesis and metal ion homeostasis imbalance hypothesis [6–8]. Currently, the main therapeutic approach in the treatment of patients with AD is to enhance the cholinergic activity in the brain. Acetylcholinesterase (AChE) and butyrylcholinesterase (BuChE) are involved in cholinergic signaling. Based on cholinergic hypothesis, the decrease in AChE levels results in a series of symptoms such as memory loss and cognitive impairment and the clinical restoration of cholinergic function is believed to alleviate AD symptoms [9,10]. Acetylcholinesterase inhibitors can inhibit the activity of acetylcholinesterase, thereby regulating the content of acetylcholine in the brain to achieve the goal in alleviating AD symptoms [11]. The drugs approved by FDA include one N-methyl-D-aspartate (NMDA) receptor antagonist and four acetylcholinesterase inhibitors, namely tacrine, donepezil, rivastigmine and galantamine [12,13]. These agents can compensate for the depletion of acetylcholine in the brain, or prevent aberrant neuronal stimulation. Nevertheless, these drugs modestly alleviate the symptoms but cannot prevent, halt or reverse the progression of AD.

Abnormal protein folding and aggregation in the brain are another important key contributing factor in the pathology of AD, and can cause neuronal damage, synaptic abnormalities and organ dysfunction [14,15]. Converging lines of evidences suggest that Amyloid-β (Aβ) tends to bunch up into small clusters and finally into the amyloid plaques, and is an important biomarker in AD. Aβ, a peptide containing 39–43 amino acid residues, has two main isoforms, Aβ (1–40) and Aβ (1–42). Aβ (1–42) shows stronger neuronal cytotoxicity and tends to aggregate more rapidly than Aβ (1–40) [16]. The potential therapy for

* Corresponding author at: School of Chemistry and Chemical Engineering, Southeast University, Nanjing, Jiangsu 211189, PR China.
E-mail address: caijin@seu.edu.cn (J. Cai).

https://doi.org/10.1016/j.bioorg.2019.03.064
Received 4 November 2018; Received in revised form 18 February 2019; Accepted 23 March 2019
Available online 28 March 2019
0045-2068/

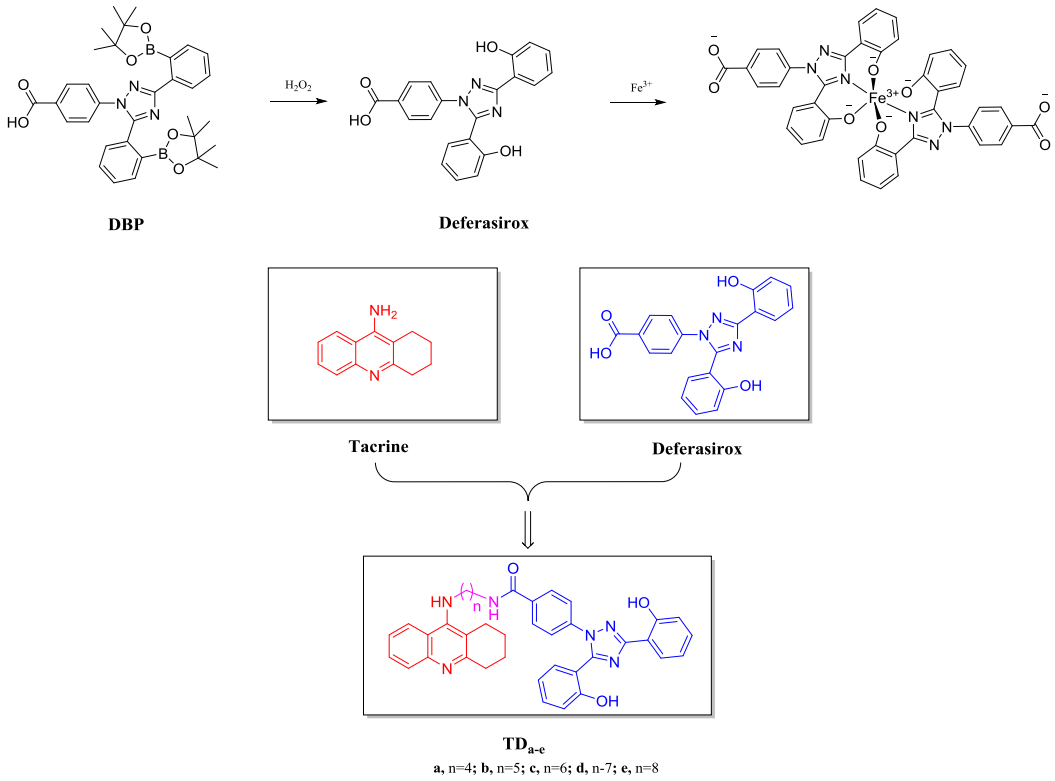

Fig. 1. Design strategy for novel compounds.

AD consists of preventing the formation and accumulation of Aβ. It has been shown, that abnormally high levels of $Cu^{+/2+}$, $Fe^{2+/3+}$ and/or Zn^{2+} lead to promote of Aβ peptide formation and generate reactive oxygen species (ROS) in AD patients [17]. Therefore, metal chelators have the ability to attenuate amyloid precursor protein (APP) expression, Aβ aggregates and neurofibrillary tangle (NFT) formation [18]. Therefore, lowering the high concentration of such metal ions in the brain by chelating the metals is an approach for the treatment of AD.

Deferasirox (**DEF**) (Fig. 1) is a bis-hydroxy-triazole tridentate iron chelator that is strongly chelating iron ions, non-toxic, and highly safe [19]. In clinic, deferasirox was used to reduce the iron overload caused by blood transfusion [20]. However, there was no effect on reducing iron ion content in the brain [21]. Deferasirox smoothly passes through the blood-brain barrier following binding to lactoferrin. Accordingly, we have prepared a new type of iron chelator **DBP** that can chelate metal ions only under oxidative stress conditions. In order to mitigate the damaging effects of metals while preserving their beneficial properties, **DBP** can be activated in the presence of H_2O_2, revealing phenolic hydroxyl groups and forming the deferasirox as shown in Fig. 1.

In view of the multiple pathogeneses of AD, the development of anti-AD drugs is moving from traditional single-target drugs to novel drugs aiming at multiple targets simultaneously including acetylcholinesterase, metal ions and free radicals which are involved in the progression of AD [22]. Tacrine (Fig. 1) is an acting anticholinesterase and was the first cholinesterase inhibitor approved by FDA for the treatment of AD [23]. Although tacrine was withdrawn due to its hepatotoxicity, its ideal pharmacokinetic properties can tolerate significant structural modifications and still maintain the inhibitory activity against AChE. In recent years, tacrine has been widely used as a lead for the development of new multifunctional agents, including tacrine-deferiprone hybrids designed by Karam et al. [24–26]. In search of new anti-AD drugs, we adopted promising drug development approaches based on multi-target directed ligands (MTLs) and then reasonably combined tacrine and deferasirox to achieve new compounds **TD**. These hybrids were anticipated to manifest AChE inhibitory activity with metal chelation and antioxidant properties [27].

2. Results and discussion

2.1. Chemistry

Based on the reported synthetic routes of boric acid ester compounds, we designed a new synthetic route for **DBP** as shown in Scheme 1. **DBP** was prepared from **DEF** via the two-step process, the triflation of phenols followed by the formation of boronate esters [28].

The key intermediates **4a–e** were synthesized as shown in Scheme 2.

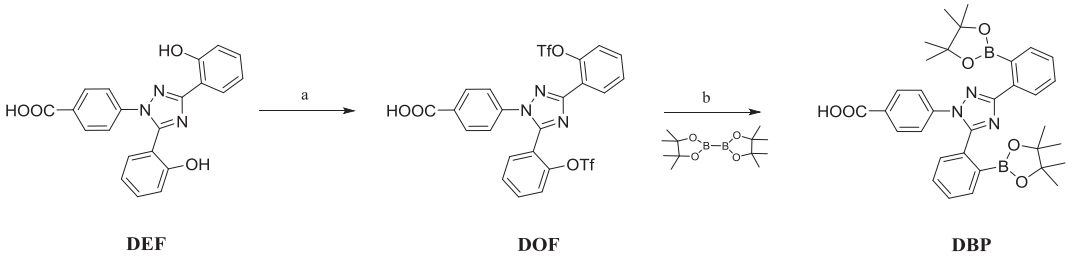

Scheme 1. (a) DIPEA, Tf_2O, DCM, −20 °C, 3 h, 85%; (b) KOAc, $PdCl_2$(dppf), DMSO, 80 °C, 24 h, 33%.

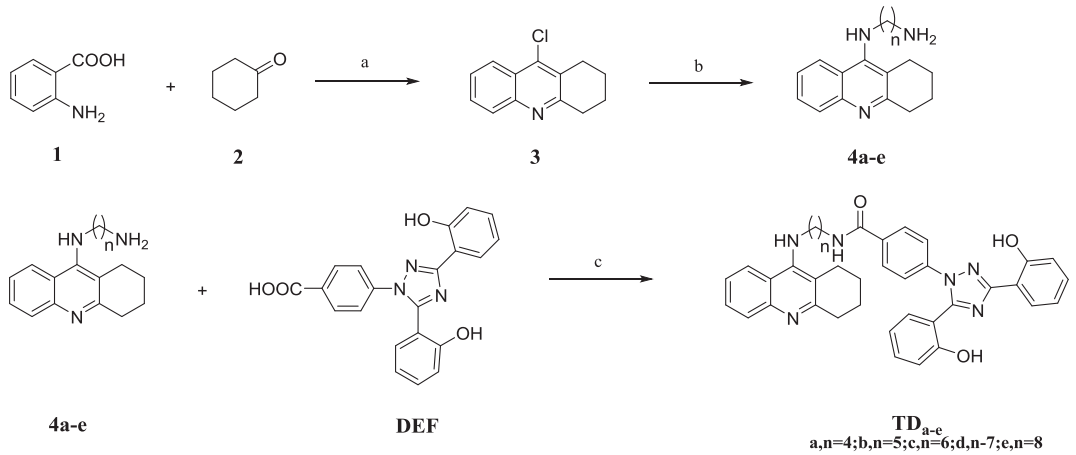

Scheme 2. (a) $POCl_3$, 3 h, 180 °C; (b) $H_2N(CH_2)_nNH_2$ (3–4 equiv), 1-pentanol, 160 °C; (c) EDCI, HOBT, Et_3N.

Compound **3** were reacted with diamines with different lengths in 1-pentanol to afford the intermediates **4a-e** [29,30]. Then, **DEF** and corresponding **4a-e** were coupled in the presence of EDCI and HOBt in DCM at room temperature to give $\mathbf{TD_{a-e}}$, respectively. Target compounds were confirmed through ^{1}H NMR, ^{13}C NMR and IR.

2.2. Metal-chelating properties of *DBP*

The chelating effect of **DBP** under oxidative stress conditions was studied with a UV–vis spectrometer and the results are shown in Fig. 2a. The peak in the absorption spectrum of **DBP** is at 304 nm. When $FeCl_3$ was added, the UV–vis absorption spectrum of **DBP** showed no obvious change. Conversely, addition of H_2O_2 to solution of **DBP** induces a significant change in spectrum, which suggests that boronate esters moieties of **DBP** is replaced with hydroxyl groups converting **DBP** to **DEF** after the addition of H_2O_2 [31]. In the presence of H_2O_2 and 0.5 equiv of $FeCl_3$, the spectrum of **DBP** showed a red shift (304 nm to 315 nm) indicating formation of the 1:2 $[Fe(\mathbf{DEF})_2]^{3-}$ complex [32]. The observations indicated that deferasirox borate ester compound has a metal chelating activity, **DBP** has no affinity for metal ions unless it is under oxidative stress condition and **DEF** serves as a metal chelator.

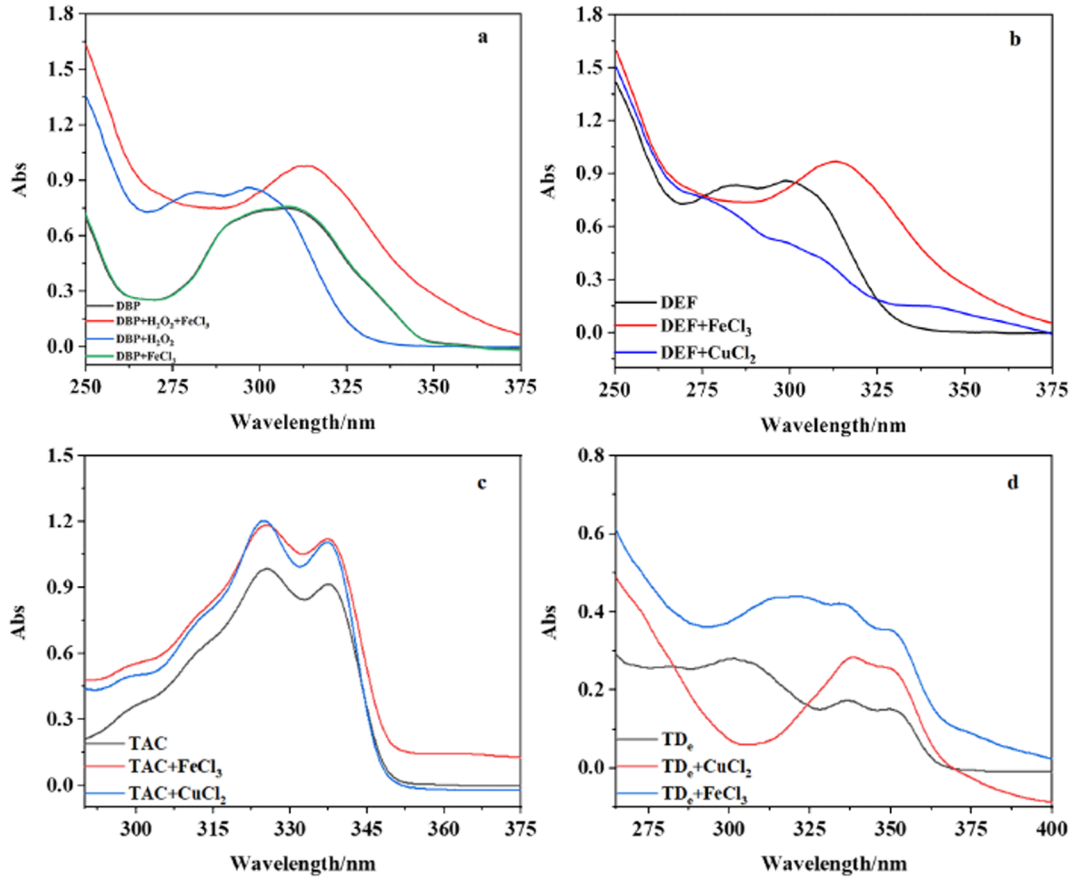

Fig. 2. The UV–vis spectra of compounds in methanol; (a) **DBP** (50 μM) alone or in the presence of $FeCl_3$ (0.5 equiv), 1.5 mM H_2O_2 and $FeCl_3$ + H_2O_2. (b) **DEF** (50 μM) alone or in the presence of $FeCl_3$ (0.5 equiv) and $CuCl_2$ (1 equiv), (c) **TAC** (40 μM) alone or in the presence of $FeCl_3$ (0.5 equiv) and $CuCl_2$ (1 equiv), (d) $\mathbf{TD_e}$ (30 μM) alone or in the presence of $FeCl_3$ (0.5 equiv) and $CuCl_2$ (1 equiv).

Table 1
Compound inhibition of bAChE activity, antioxidant activity and CLogP value prediction.

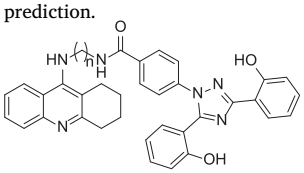

TD_{a-e}

Compound	n[a]	IC_{50}[b] (μM) bAChE[b]	Antioxidant activity[c] (%)	CLogP
TD_a	4	13.5 ± 0.82	32 ± 0.23	6.996
TD_b	5	17.8 ± 0.21	34 ± 0.56	6.909
TD_c	6	15.4 ± 0.27	39 ± 0.42	7.315
TD_d	7	16.1 ± 0.36	49 ± 0.31	7.297
TD_e	8	13.7 ± 0.21	56 ± 0.69	7.265
Tacrine		14.1 ± 0.33	–	–
DEF		–	23 ± 0.52	3.688

[a] Carbon length.
[b] All values are expressed as mean ± SEM from three independent experiments.
[c] bAChE from bovine serum.

2.3. Pharmacological activity of *TD* compounds

2.3.1. Cholinesterase inhibitory activity

The inhibitory activities of hybrid **TD** compounds against AChE from bovine serum (bAChE) were determined by the ELISA method [33]. Bovine serum AChE shows a high degree of homology with the corresponding human enzymes and it has more availability from commercial sources, making it a reasonable alternative [34]. For comparison purpose, tacrine was used as a reference compound. The IC_{50} values of all test compounds were summarized in Table 1. As shown in Table 1, all new target compounds displayed inhibitory activities against bAChE with micromolar IC_{50} values, which were virtually the same inhibitory activities as that of tacrine. The introduction of the **DEF** scaffold to tacrine with linkers with various lengths did not alter the potency of tacrine. Among the target compounds, **TD_a** (IC_{50} = 13.5 μM) and **TD_e** (IC_{50} = 13.7 μM) showed the slightly better potent inhibitory activity for bAChE.

2.3.2. Molecular modeling study

To further study the possible binding modes of **TD** derivatives in AChE, a molecular docking study with *Torpedo californica* variant of AChE (*Tc*AChE) (PDB ID: 2CMF) was performed using Glide [35]. As shown in Fig. 3, the tacrine moiety of **TD_a** occupies the catalytic active site (CAS) of *Tc*AChE, forming π-π stacking interactions with Phe 330 and Trp 84. The N atom of quinoline ring also forms a water-mediated H-bond with His 440. The long alkyl linker is located in the mid-gorge region of *Tc*AChE and has no interactions with the amino acid residues. The deferasirox moiety of **TD_a** occupies the peripheral anionic site (PAS) of *Tc*AChE, via a π-π interaction with Trp 279 and the hydroxyl via H-bonding interactions with Trp 279 and Tyr 334. The docking results indicate that new **TD** compounds could simultaneously bind to the CAS and PAS of *Tc*AChE, demonstrating the rationale of our design. The new tacrine hybrids inhibitory activities for *Tc*AChE were no significantly improvement, as compared with tacrine, which might be due to their chain length and steric hindrance, similarly to previous report for the same linker in other tacrine hybrids [36].

2.3.3. Cytotoxicity and effect on H_2O_2-induced oxidative cell damage in PC12

To examine the cytotoxicity of **TD** compounds, cell viability was assayed using the rat pheochromocytoma cell line PC12 [37,38], and tested using the 3-(4,5- dimethylthiazol-2-yl)-2,5- diphenyltetrazolium (MTT) assays [39]. PC12 cells were treated with **TD_a**, **TD_b**, **TD_c**, **TD_d** and **TD_e** at three different concentrations (3, 5 and 10 μM) for 24 h. H_2O_2 (150 μM) was used to induce oxidative damage, and **DEF** and tacrine were included as reference compounds. As shown in Fig. 4, the treatment of P12 cells with compound **DEF** did not show any change in the cell viability compared to the control treated with only H_2O_2. Tacrine was potent in protecting cell damage manifesting the cell viability of 92.6% at 10 μM, but it did not exert the cell protective activity against the injury caused by H_2O_2. At 10 μM concentration, **TD_a** or **TD_b** manifested a decrease of cell viability (21.4% and 29.4%, respectively). The viability of cells treated with **TD_a** or **TD_b** further decreased to 9.1% and 21.4%, respectively, when H_2O_2 was added. Compound **TD_e** exhibited a good protective activity for PC12 cells damaged by oxidative stress at 10 μM with cell viability of 64.4% and 68.1% in the presence and absence of H_2O_2, respectively. These results showed that cytotoxicity was significantly reduced as the length of the alkyl linker increased and this result deserved a further study.

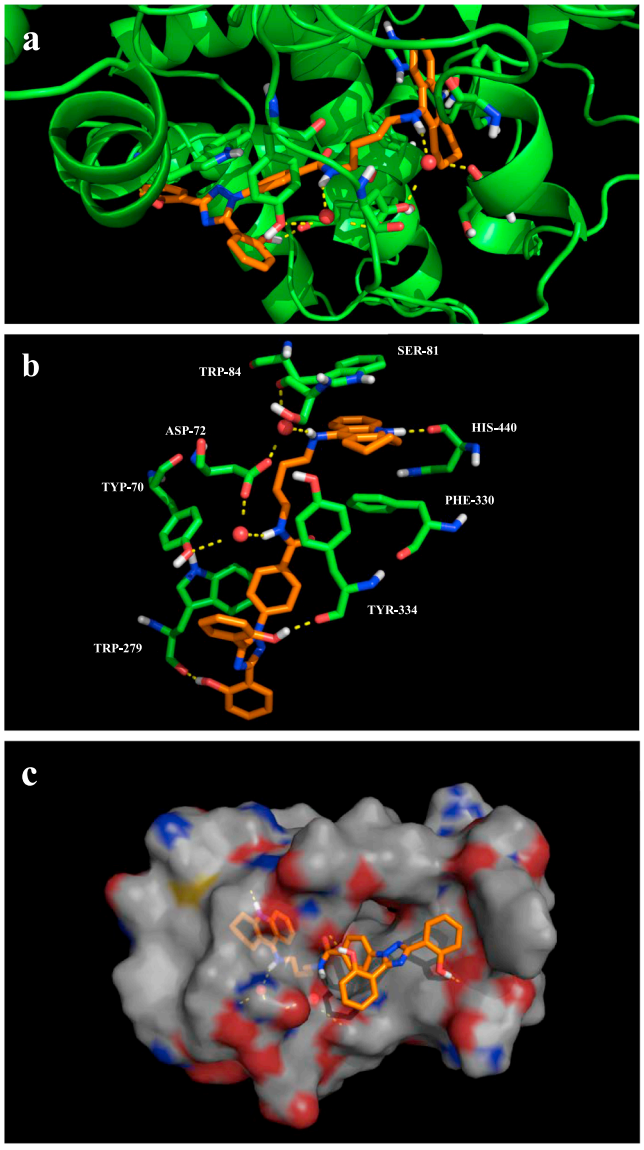

Fig. 3. Docking models of the **TD_a** in *Torpedo californica* AChE (PDB code: 2CMF). The dashed lines represent the interactions between the AChE and the ligand: (a) 3D docking image of compound **TD_a** with AChE, (b) interactions between the binding sites of compounds **TD_a** and AChE, (c) docking compound **TD_a** in the surface model of AChE.

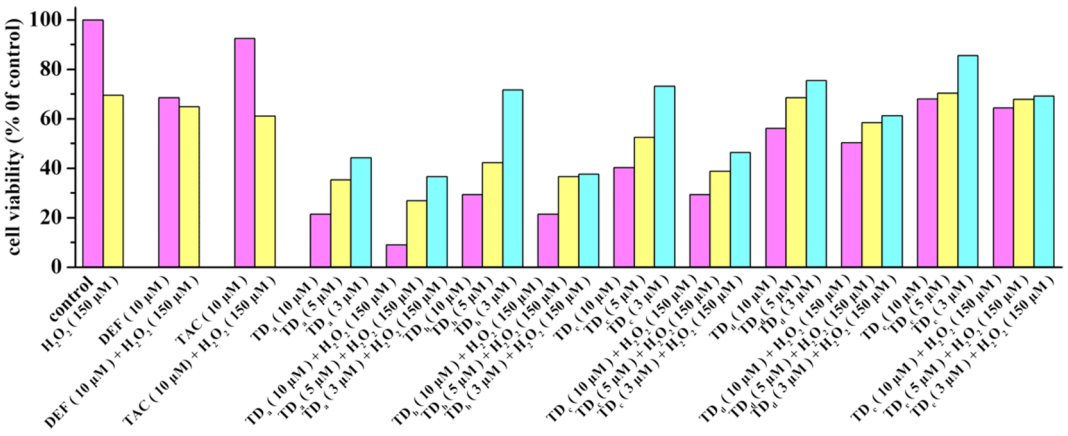

Fig. 4. Effect of **TD_a**, **TD_b**, **TD_c**, **TD_d** and **TD_e** on H_2O_2-induced oxidative cell damage in PC12 cells.

2.3.4. DPPH free radical scavenging activity

To further study, free radical scavenging activities of **TD** compounds was evaluated using the DPPH assay [40]. As shown in Table 1, it was observed that **TD_e** exhibited more profound radical scavenging effect and **TD_c**, **TD_d** were found to exhibit moderate antioxidant activity. The radical scavenging capacity of new compounds results from the hydroxyl group of **DEF** and the length of linker [26].

2.3.5. In vitro blood–brain barrier permeation assay

For successful central nervous system (CNS) drugs, it is important that the compounds are able to cross the blood–brain barrier (BBB). The 'rule of 5' predicts that good absorption or permeation is more likely when there are less than 5 H-bond donors, 10 H-bond acceptors, the molecular weight (MW) is less than 500 and the calculated LogP (CLogP) is less than 5 (or MLogP < 4.15) [41]. To evaluate the potential of these hybrids to cross the BBB, we calculated CLogP values using the ChemDraw 17.0. From Table 1, the CLogP value of five compounds (**TD_a**, **TD_b**, **TD_c**, **TD_d** and **TD_e**) were all greater than 5, indicating that **TD** compounds might be difficult to penetrate the BBB. Therefore, we consider using nanoparticles or liposomes as carriers to enable drugs to cross the blood-brain barrier in the future.

*2.3.6. Metal-chelating properties of compound **TD_e***

As compound **TD_e** showed a favorable antioxidant activity and a bAChE inhibitory activity with IC_{50} of 13.7 μM, its metal-chelating ability was investigated. The chelating abilities of compounds **DEF**, **TAC** and **TD_e** with 0.5 equiv of Fe^{3+} and 1 equiv of Cu^{2+} were studied using the UV–vis spectrometric method are shown in Fig. 2b–d (respectively). When $FeCl_3$ or of $CuCl_2$ was added, the UV–vis spectrum of **TAC** showed no obvious change, indicating that **TAC** did not chelate metal ions. Upon the addition of $FeCl_3$ to **DEF**, a red shift of the maximum absorption from 295 nm to 315 nm, suggesting the formation of the $[Fe(DEF)_2]^{3-}$ complex. The results were similar to a previous report for UV–vis spectra of **DEF** [32]. When $CuCl_2$ was added, a significant change could be observed, which was similar to reported **DEF**-Cu^{2+} complex [42]. Similarly, the addition of Fe^{3+} or Cu^{2+} to **TD_e** resulted in the shifts from 305 nm to 324 nm (for Fe^{3+}) or 338 nm (for Cu^{2+}). The complexation ability of **TD_e** might be ascribed to **DEF** moiety of the compound.

3. Conclusions

In conclusion, we designed and synthetized tacrine-deferasirox compounds as multifunctional agents against AD. The new hybrids combined the capacities of *Tc*AChE inhibition of tacrine and chelate metal ability of deferasirox. In all new compounds, **TD_a** and **TD_e** displayed the inhibitory activity against bAChE with IC_{50} values of 13.5 μM and 13.7 μM, respectively, which were virtually the same inhibitory activities as that of tacrine. Molecular modeling studies indicated that new **TD** compounds could simultaneously occupy the CAS and PAS of *Tc*AChE. Moreover, **TD_e** exhibited the low cytotoxicity and effectively cell protective activity for the injury caused by H_2O_2. Furthermore, **TD_e** was found a more profound radical scavenging effect than **DEF** and was able to bind Fe^{3+} and Cu^{2+} to form chelate metal complexes. In addition, new compound **DBP** could serve as a metal chelator under an oxidative stress condition. It suggests that **DBP** will facilitate management metal burden at locations of disease without stimulating widespread metal redistribution. Moreover, such multifunctional properties indicated that **TD_e** as a novel multi-target cholinesterase inhibitor and **TD** compounds could be considered as promising compounds for the further study in development of anti-AD drugs.

4. Experimental section

4.1. Chemistry

All chemicals (reagent grade) were obtained from commercial suppliers and used without further purification. Reaction progress was monitored by thin-layer chromatography (TLC) using silica gel GF_{254} plates from Qingdao Haiyang Chemical Plant (China) and the spots were detected under UV light (254 nm). Melting points were measured on RY-1 melting-point instrument (China) and are uncorrected. Column chromatography using silica gel (200–300 mesh) purchased from Qingdao Haiyang Chemical Plant (China). ^1H NMR and ^{13}C NMR spectra were measured on a Bruker Avance DPX-300/500 spectrometer at 25 °C and referenced to tetramethylsilane (TMS) by China Pharmaceutical University Analytical Testing Center. IR (FI-IR) spectra were recorded on a Perkin-Elmer spectrometer by Suzhou Southeast Pharmaceutical Co., Ltd. (China).

*4.1.1. 4-(3,5-Bis(2-(((trifluoromethyl)sulfonyl)oxy)phenyl)-1H-1,2,4-triazol-1-yl)benzoic acid (**DOF**)*

To a stirred solution of **DEF** (0.73 g, 1 mmol) and a few drops of DMF in dry CH_2Cl_2 at −20 °C was added dropwise *N,N*-diisopropylethylamine (0.006 mmol) and trifluoromethanesulfonic anhydride (0.006 mmol) in 40 min. The reaction mixture was stirred for 4 h at room temperature and quenched in ice-cold water, filtered and washed with water, brine and dried (Na_2SO_4). Evaporation of the solvent give (**DOF**) as a yellow oil which was used in the next step without further purification. ^1H NMR (500 MHz, DMSO-d_6) δ: 8.26–8.15 (m, 4H), 7.69–7.54 (m, 4H), 7.14–7.01 (m, 4H); MS: $[M-H]^-$ *m/z* calcd 635.9975 for $C_{23}H_{13}F_6N_3O_8S_2$, found 636.9975.

*4.1.2. 4-(3,5-Bis(2-(4,4,5,5-tetramethyl-1,3,2-dioxaborolan-2-yl)phenyl)-1H-1,2,4-triazol-1-yl)benzoic acid (**DBP**)*

A mixture of **DOF**, potassium acetate (0.54 g, 5.46 mmol), bis(pinacolato)diboron (0.26 g, 5.46 mmol) and catalytic $PdCl_2$(dppf) in DMSO was heated at 80 °C under N_2 atmosphere for 24 h. The mixture was cooled to RT, diluted with ethyl acetate and washed with water, brine and dried (Na_2SO_4). The residue was purified by silica gel chromatography to yield the desired (**DBP**) as a yellow solid (0.19 g, 33% yield). mp 178.2–179.5 °C; ^{1}H NMR (300 MHz, CD_3OD) δ: 1.25 (m, 21H), 2.25 (m, 3H), 6.92 (m, 4H), 7.39 (m, 4H), 8.08 (m, 4H); ^{13}C NMR (75 MHz, DMSO-d_6) δ:116.27, 154.95, 151.15, 150.12, 148.59, 138.36, 133.34, 132.34, 130.33, 129.96, 128.99, 128.60, 128.55, 126.40, 126.36, 126.32, 123.74, 117.98, 83.90, 25.07; IR (KBr, cm^{-1}): 3412.9, 3365.9 (C═C), 2977.9 (C−H), 2736.1 (N═N), 1686, 1606.3, 1561.5, 1532.5, 1481, 1446.1, 974.9, 959.9, 849.6; MS: $[M+H]^+$ *m/z* calcd 594.2941 for $C_{33}H_{37}B_2N_3O_6$, found 594.2943.

*4.1.3. 9-Chloro-1,2,3,4-tetrahydroacridine (**3**)*

To an ice-cooled solution of anthranilic acid (3.2 g, 3 mmol) and cyclohexanone (2.65 mL, 27 mmol) was added dropwise $POCl_3$ with a constant pressure dropping funnel. Then, the reaction was heated at reflux for 3 h. The solvent was reduced in vacuum and the residue was dissolved in ethyl acetate and washed with 1 N K_2CO_3 solution, brine and dried (Na_2SO_4). The residue was purified by silica gel chromatography to yield the desired (**3**) as a yellow solid (4.6 g, 91% yield). mp 67.2–69.2 °C.

*4.1.4. General procedure for the synthesis of intermediates **4a-e***

A mixture of compound **3** (1.0 g, 3.61 mmol) and different amines (13.8 mmol) in 1-pentanol (5 mL) was stirred at 160 °C for 36 h until TLC revealed completion of the reaction. The mixture was diluted with DCM, filtered and the filtrate was washed with water, 1 N NaOH solution, brine and dried (Na_2SO_4). The crude was reduced in vacuum and the residue purified by silica gel chromatography to yield the desired (**4a-e**), respectively.

*4.1.4.1. N^1-(1,2,3,4-tetrahydroacridin-9-yl)butane-1,4-diamine (**4a**)*. Brown oil; 71% yield; ^{1}H NMR (300 MHz, $CDCl_3$) δ: 1.08 (s, 2H), 1.28 (d, J = 7.4 Hz, 2H), 1.45 (d, J = 7.4 Hz, 2H), 2.49–2.54 (m, 4H), 2.87 (t, J = 6.0 Hz, 2H), 3.25 (t, J = 7.1 Hz, 2H), 3.89–3.95 (m, 4H), 7.13 (t, J = 7.6 Hz, 1H), 7.35 (t, J = 7.6 Hz, 1H), 7.75 (t, J = 8.4 Hz, 2H); MS: $[M-H]^-$ *m/z* calcd 268.1819 for $C_{17}H_{23}N_3$, found 268.1910.

*4.1.4.2. N^1-(1,2,3,4-tetrahydroacridin-9-yl)pentane-1,5-diamine (**4b**)*. Brown oil; 89% yield; ^{1}H NMR (300 MHz, $CDCl_3$) δ: 1.26–1.33 (m, 2H), 1.35–1.42 (m, 2H), 1.54 (d, 2H, J = 7.3 Hz), 1.79 (d, J = 3.3 Hz, 4H), 2.24 (s, 2H), 2.53 (s, 2H), 2.61 (s, 2H), 2.91(s, 2H), 3.24 (t, 2H, J = 7.2 Hz), 3.87 (s, 1H), 7.13 (dd, J = 9.0, 2.2 Hz, 1H), 7.76 (d, J = 9.0 Hz, 1H), 7.77 (d, J = 2.2 Hz, 1H); MS: $[M+H]^+$ *m/z* calcd 284.2121 for $C_{18}H_{25}N_3$, found 284.2012.

*4.1.4.3. N^1-(1,2,3,4-tetrahydroacridin-9-yl)hexane-1,6-diamine (**4c**)*. Yellow oil; 56% yield; ^{1}H NMR (300 MHz, $CDCl_3$) δ: 1.35–1.39 (m, 6H), 1.59–1.64 (m, 4H), 1.85–1.96 (m, 4H), 2.61–2.73 (m, 4H), 3.01–3.67 (m, 2H), 3.41 (t, J = 7.1 Hz, 2H), 3.89 (s, 1H), 7.28 (t, J = 7.6 Hz, 1H), 7.49 (t, J = 7.6 Hz, 1H), 7.85 (d, J = 8.6 Hz, 1H), 7.90 (d, J = 8.5 Hz, 1H); MS: $[M+H]^+$ *m/z* calcd 298.2277 for $C_{19}H_{27}N_3$, found 298.2272.

*4.1.4.4. N^1-(1,2,3,4-tetrahydroacridin-9-yl)heptane-1,7-diamine (**4d**)*. Brown oil; 71% yield; ^{1}H NMR (300 MHz, CD_3OD) δ: 1.24–1.47 (m, 8H), 1.52 (d, J = 7.2 Hz, 2H), 1.64 (d, J = 7.2 Hz, 2H), 1.86–1.90 (m, 4H), 2.70–2.78 (m, 6H), 2.93–2.95 (m, 2H), 3.55 (t, J = 7.2 Hz, 2H), 7.34(ddd, J = 1.1, 7.2, 8.7 Hz, 1H), 7.56 (d, J = 6.9 Hz, 1H), 7.74 (dd, J = 0.8, 8.7 Hz, 1H), 8.10 (dd, J = 0.8, 8.6 Hz, 1H); MS: $[M+H]^+$ *m/z* calcd 312.2434 for $C_{20}H_{29}N_3$, found 312.2442.

*4.1.4.5. N^1-(1,2,3,4-tetrahydroacridin-9-yl)octane-1,8-diamine (**4e**)*. Brown oil; 76% yield; ^{1}H NMR (300 MHz, CD_3OD) δ: 1.31 (s, 8H), 1.55–1.69 (m, 4H), 1.88–1.91 (m, 4H), 2.71 (s, 2H), 2.83 (t, J = 7.6 Hz, 2H), 2.98 (s, 2H), 3.67 (t, J = 7.2 Hz, 2H), 7.42 (ddd, J = 1.4, 7.0, 8.4 Hz, 1H), 7.64 (d, J = 6.9 Hz, 1H), 7.76 (d, J = 8.6 Hz, 1H), 8.18 (d, J = 8.5 Hz, 1H); MS: $[M+H]^+$ *m/z* calcd 326.2590 for $C_{21}H_{31}N_3$, found 326.2597.

*4.1.5. General procedure for the synthesis of **TD$_{a-e}$***

To an ice-cooled solution of **DEF** (0.373 g, 1 mmol), HOBT (0.2 g 1.5 mmol) and EDCI (0.2 g, 1.5 mmol) in DMF was stirred for 1 h. Then, compound **4a-e** was added and the mixture was stirred at room temperature for 6 h until TLC revealed completion of the reaction. The mixture was diluted with DCM, filtered and the filtrate was washed with water, brine and dried (Na_2SO_4). The crude was reduced in vacuum and the residue purified by silica gel chromatography to yield the desired (**TD$_{a-e}$**), respectively.

*4.1.5.1. 4-(3,5-Bis(2-hydroxyphenyl)-1H-1,2,4-triazol-1-yl)-N-(4-((1,2,3,4-tetrahydroacridin-9-yl)amino)butyl)benzamide (**TD$_a$**)*. Yellow solid; 33% yield; mp 147.3–148.5 °C; ^{1}H NMR (300 MHz, DMSO-d_6) δ: 1.05 (t, J = 5.73 Hz, 2H), 1.59 (t, J = 8.94 Hz, 4H), 2.71 (d, J = 5.73 Hz, 2H), 2.88 (d, J = 5.19 Hz, 2H), 3.22–3.28 (m, 2H), 3.46–3.52 (m, 2H), 5.75 (s, 1H), 6.88 (d, J = 8.22 Hz, 1H), 6.95–7.04 (m, 3H), 7.35 (t, J = 7.95 Hz, 3H), 7.49–7.57 (m, 4H), 7.70 (d, J = 8.34 Hz, 1H), 7.84 (d, J = 8.43 Hz, 2H), 8.05 (d, J = 7.47 Hz, 1H), 8.14 (d, J = 8.58 Hz, 2H), 8.50 (t, J = 5.04, 1H), 10.20 (s, 1H), 10.79 (s, 1H); ^{13}C NMR (75 MHz, DMSO-d_6) δ: 168.55, 162.63, 158.14, 157.92, 157.60, 154.33, 150.50, 148.11, 147.71, 132.70, 132.47, 131.58, 129.88, 129.69, 129.02, 128.25, 125.45, 125.38, 124.76, 124.30, 123.25, 120.79, 120.00, 117.82, 117.27, 116.23, 114.59, 111.25, 43.82, 37.78, 32.69, 27.54, 27.14, 26.04, 22.78, 22.02; IR (KBr, cm^{-1}): 3425.5, 3373.9 (C═N), 3059.1 (O−H), 2927.9 (C−H), 2534.2 (N═N), 1650, 1608.4, 1572.3 (C═C), 1510.1, 1462.4, 858.3, 754.3; MS: $[M+H]^+$ *m/z* calcd 625.2921 for $C_{38}H_{36}N_6O_3$, found 625.2927.

*4.1.5.2. 4-(3,5-Bis(2-hydroxyphenyl)-1H-1,2,4-triazol-1-yl)-N-(5-((1,2,3,4-tetrahydroacridin-9-yl)amino)pentyl)benzamide (**TD$_b$**)*. Yellow solid; 59% yield; mp 140.1–141.2 °C. ^{1}H NMR (300 MHz, $CDCl_3$) δ: 1.49 (t, J = 7.05 Hz, 2H), 1.63–1.74 (m, 4H), 1.88 (s, 4H), 2.68 (s, 2H), 2.96 (s, 2H), 3.44–3.54 (m, 4H), 3.99 (d, J = 5.88 Hz, 1H), 6.34 (s, 1H), 6.71 (t, J = 7.56 Hz, 1H), 6.99–7.09 (m, 4H), 7.26–7.39 (m, 4H), 7.48–7.56 (m, 3H), 7.79–7.94 (m, 4H), 8.13 (d, J = 7.71 Hz, 1H); ^{13}C NMR (75 MHz, DMSO-d_6) δ: 167.89, 162.63, 158.14, 157.92, 157.60, 154.33, 150.50, 148.11, 144.28, 132.70, 132.57, 131.19, 129.87, 129.69, 129.02, 128.25, 125.45, 125.38, 124.76, 124.31, 123.25, 120.79, 120.00, 117.82, 117.21, 116.23, 112.50, 111.24, 43.90, 36.67, 32.69, 29.80, 29.18, 24.68, 24.14, 22.94, 22.02; IR (KBr, cm^{-1}): 3270.3 (C═N), 3190.4, 3055.7 (O−H), 2929.3 (C═H), 2857.2, 2547.7 (N═N), 2491, 1643.5, 1609.5, 1583.6, 1504, 1462.2, 855, 830.5, 754.9; MS: $[M+H]^+$ *m/z* calcd 639.3078 for $C_{39}H_{38}N_6O_3$, found 639.3071.

*4.1.5.3. 4-(3,5-Bis(2-hydroxyphenyl)-1H-1,2,4-triazol-1-yl)-N-(6-((1,2,3,4-tetrahydroacridin-9-yl)amino)hexyl)benzamide (**TD$_c$**)*. Yellow solid; 50% yield; mp 120.3–122.2 °C; ^{1}H NMR (300 MHz, $CDCl_3$) δ: 0.83–0.89 (m, 3H), 1.43 (s, 5H), 1.88 (s, 4H), 2.67 (s, 2H), 2.98 (s, 2H), 3.44–3.52 (m, 4H), 4.13 (s, 1H), 6.40 (s, 1H), 6.69 (t, J = 7.53 Hz, 1H), 6.99–7.09 (m, 4H), 7.30–7.39 (m, 3H), 7.49–7.56 (m, 3H), 7.83–7.97 (m, 4H), 8.13 (d, J = 7.62 Hz, 1H); ^{13}C NMR (75 MHz, DMSO-d_6) δ: 168.13, 162.63, 160.41, 156.96, 156.79, 154.33, 150.29, 148.91, 145.79, 132.63, 132.54, 131.48, 129.94, 129.69, 129.11, 128.15, 125.59, 125.38, 124.81, 124.46, 123.18, 120.79, 119.84, 117.82, 117.61, 116.23, 114.59, 112.26, 44.00, 37.38, 32.69, 30.64, 29.82, 27.11, 24.68, 22.41, 20.60; IR (KBr, cm^{-1}): 3270.3, 3192.3, 3055.6,

2967.9, 2930.1 (C—H), 2547.8, 2491, 1642.5, 1609.6, 1563.6, 1504.1, 1462.2, 855.2, 830.5, 754.8; MS: $[M+H]^+$ *m/z* calcd 653.3234 for $C_{40}H_{40}N_6O_3$, found 653.3237.

*4.1.5.4. 4-(3,5-Bis(2-hydroxyphenyl)-1H-1,2,4-triazol-1-yl)-N-(7-((1,2,3,4-tetrahydroacridin-9-yl)amino)heptyl)benzamide (**TD$_d$**).* Yellow solid; 57% yield; mp 117.1–118.5 °C. ^{1}H NMR (300 MHz, $CDCl_3$) *δ*: 1.26–1.36 (m, 6H), 1.56–1.64 (m, 4H), 1.89 (s, 4H), 2.69 (s, 4H), 2.99 (s, 2H), 3.40–3.51 (m, 4H), 4.00 (s, 1H), 6.35 (s, 1H), 6.70 (t, *J* = 7.65 Hz, 1H), 7.00–7.08 (m, 4H), 7.29–7.39 (m, 3H), 7.49–7.59 (m, 3H), 7.80 (d, *J* = 8.10 Hz, 1H), 7.94 (t, *J* = 8.10 Hz, 3H), 8.14 (d, *J* = 7.74 Hz, 1H); ^{13}C NMR (75 MHz, DMSO-d_6) *δ*: 169.97, 163.73, 160.55, 157.92, 157.75, 154.14, 150.46, 148.26, 144.28, 132.73, 132.38, 131.58, 130.14, 129.75, 128.87, 128.03, 126.80, 126.59, 124.96, 124.30, 122.11, 120.88, 120.30, 117.82, 117.27, 116.23, 114.15, 111.44, 45.10, 36.36, 32.93, 31.05, 29.55, 28.49, 26.91, 26.75, 24.78, 23.07, 21.32; IR (KBr, cm^{-1}): 3352.1, 3271.1, 3060.9, 2926, 2853.7, 2488, 1920, 1738.4, 1608.9, 1581.2, 1504.5, 1463.2, 854.7, 830.7, 752.4; MS: $[M+H]^+$ *m/z* calcd 667.3391 for $C_{41}H_{42}N_6O_3$, found 667.3395.

*4.1.5.5. 4-(3,5-bis(2-hydroxyphenyl)-1H-1,2,4-triazol-1-yl)-N-(8-((1,2,3,4-tetrahydroacridin-9-yl)amino)octyl)benzamide (**TD$_e$**).* Yellow solid; 60% yield; mp 112.7–113.5 °C; ^{1}H NMR (300 MHz, $CDCl_3$) *δ*: 1.06 (t, *J* = 7.11 Hz, 6H), 1.57–1.66 (m, 5H), 1.89 (s, 4H), 2.54–2.61 (m, 3H), 2.69 (s, 2H), 3.00 (s, 2H), 3.43–3.50 (m, 4H), 4.02 (s, 1H), 6.39 (s, 1H), 6.70 (t, *J* = 7.59 Hz, 1H), 7.00–7.08 (m, 4H), 7.33–7.7.39 (m, 3H), 7.49–7.59 (m, 3H), 7.80 (d, *J* = 8.34 Hz, 1H), 7.94 (d, *J* = 8.07 Hz, 3H), 8.14 (d, *J* = 7.65 Hz, 1H); ^{13}C NMR (75 MHz, DMSO-d_6) *δ*: 169.10, 162.65, 158.57, 157.68, 157.61, 154.33, 151.01, 148.62, 145.23, 132.47, 132.33, 131.58, 129.92, 129.53, 128.87, 128.25, 125.45, 124.12, 123.07, 122.89, 119.82, 117.62, 117.13, 115.55, 114.06, 111.64, 44.22, 37.17, 32.69, 30.64, 29.82, 27.47, 26.91, 24.68, 22.94, 22.34; IR (KBr, cm^{-1}): 3276.2, 3190.9, 3057.9, 2929.8, 2855.9, 2547.3, 1913.5, 1830.8, 1609.9, 1504.2, 1462.5, 855.2, 830.6, 754.9; MS: $[M+H]^+$ *m/z* calcd 681.3547 for $C_{42}H_{44}N_6O_3$, found 681.3577.

4.2. Biological evaluation

4.2.1. Metal binding studies

The study of metal chelation was performed in methanol at 298 K using UV–vis spectrophotometer (Shanghai Csoif Co., Ltd) with wavelength ranging from 200 to 500 nm. To investigate whether **DBP**, **TD$_e$** and **DEF** could chelate metals, the UV absorption tested in the absence or presence of metal ion. Stock solutions of **DBP** (2.5 mM), **DEF** (2.5 mM), **TAC** (2 mM) and **TD$_e$** (1.5 mM) were eventually diluted 50 times with methanol. Metal salt solutions of $FeCl_3$ (10 mM) and $CuCl_2$ (10 mM) were prepared in water. The solutions were incubated for 1 h with 0.5 equiv of Fe^{3+}, 1 equiv of Cu^{2+} or 2 mM H_2O_2 before UV–Vis spectra were recorded.

4.2.2. Inhibition experiments of bAChE

AChE activities were measured by ELISA method with using AChE from bovine serum (bAChE) [43]. Double antibody sandwich assay used to determine the activities of bAChE by the microplate was coated with purified bAchE antibody to prepare a solid phase antibody, and AchE was sequentially added to the microplate, followed by HRP-labeled AChE. Combines to form an antibody-antigen-enzyme-labeled antibody complex, which is thoroughly washed and TMB was added and turned from blue to yellow under the action of acid. Follow the cattle (AChE) ELISA kit instructions (Shanghai Du Yi biology Co., Ltd.), on the enzyme label coating plate, 40 μL of biological reference preparation (120 U/L, 80 U/L, 40 U/L, 20 U/L and 10 U/L) was incubated with different test compounds (10 μL) at 37 °C for 30 min followed by the enzyme standard reagent (50 μL) and the absorbance was measured at a wavelength of 450 nm in 15 min. The concentration of compound producing 50% of enzyme activity inhibition (IC_{50}) was calculated by linear regression analysis using the Origin 8.0 program package. Tacrine were purchased from Shanghai Zhen Zhi Biological Technology Co., Ltd. positive drug and all samples were assayed in triplicate.

4.2.3. Molecular modeling study

Molecular modeling calculations and docking studies were performed using Schrodinger's software Glide-Docking. The X-ray crystallographic structures of *Torpedo californica* AChE complexed with bis (5)-tacrine (PDB code 2CMF) was obtained from the Protein Data Bank [35]. All water molecules in PDB files were removed and hydrogen atoms were subsequently added to the protein. The compound **TD$_a$** was built and performed geometry optimization by molecular mechanics. Then, the **TD$_a$** was docked into the active site of the protein by using Glide 6.7 program with default parameters [44,45]. Docking accuracy is Standard Precision (SP) and the dock scoring in Glide software was done using Glide score function. After docking, the geometry of resulting complex was studied using the Glide's pose viewer.

4.2.4. Effect on H_2O_2-induced oxidative cell damage in PC12 cells

The rat pheochromocytoma PC12 cells were routinely grown at 37 °C in a humidified incubator with 5% CO_2 and were plated at a density of 3×10^3 cells/well on 96-well plates in 100 μL of DMEM. Compounds **TD$_a$**, **TD$_b$**, **TD$_c$**, **TD$_d$** and **TD$_e$** were dissolved with 150 μL DMSO first, and then diluted with PBS. The cells were pre-incubated with compounds for 24 h before H_2O_2 (150 μM) was added. The cells were treated without H_2O_2 for 3 h, and cell viability was determined after replaced with fresh DMEM medium. The cells were treated with 50 μL MTT for 4 h at 37 °C. The absorption was measured by a well plate reader at 490 nm.

4.2.5. DPPH scavenging activity

DPPH radical scavenger solution in methanol showed a maximum absorption wavelength at 517 nm (Fig. S1). The test compound was formulated into10^{-1}, 10^{-2}, 10^{-3}, 10^{-4}, 10^{-5} and 10^{-6} **M** solution, then 2.5 mL of DPPH solution was added separately. The mixture treated for 30 min at room temperature, the absorbance of the solution with different concentrations at 517 nm was obtained. The antioxidant activity was computed according to equation shown below:

$$AA\% = A_{DPPH} - A_{sample}/A_{DPPH}$$

AA% indicates the antioxidant activity of a compound, A_{DPPH} indicates the absorbance of pure DPPH methanol solution, and A_{sample} indicates the absorbance of a tested compound.

4.2.6. In vitro blood–brain barrier permeation prediction

To evaluate the potential for these hybrids to cross the BBB, we predict CLogP values by ChemDraw 17.0. The CLogP values of compound was studied in the chemical properties window.

Acknowledgments

This work was supported by Jiangsu Natural Science Foundation (BK20161438), the Southeast University's Basic Research Business Fee Innovation Foundation (3207048416).

Appendix A. Supplementary material

Supplementary data to this article can be found online at https://doi.org/10.1016/j.bioorg.2019.03.064.

References

[1] H. Tang, H.T. Zhao, S.M. Zhong, Z.Y. Wang, Z.F. Chen, H. Liang, Novel oxoisoaporphine-based inhibitors of acetyl-and butyrylcholinesterase and

acetylcholinesterase-induced β-amyloid aggregation, Bioorg. Med. Chem. Lett. 22 (6) (2012) 2257–2261.
[2] Y. Rook, K.U. Schmidtke, F. Gaube, D. Schepmann, B. Wuensch, J. Heilmann, J. Lehmann, T. Winckler, Bivalent β-carbolines as potential multitarget anti-alzheimer agents, J. Med. Chem. 53 (9) (2010) 3611–3617.
[3] K. Bettens, K. Sleegers, C. Van Broeckhoven, Current status on Alzheimer disease molecular genetics: from past, to present, to future, Hum. Mol. Genet. 19 (R1) (2010) R4–R11.
[4] A. Wimo, L. Jonsson, J. Bond, M. Prince, B. Winblad, I. Alzheimer Dis, The worldwide economic impact of dementia 2010, Alzheimers Dementia 9 (1) (2013) 1–11.
[5] E.D. Roberson, L. Mucke, 100 years and counting: prospects for defeating Alzheimer's disease, Science 314 (5800) (2006) 781–784.
[6] C.X. Gong, K. Iqbal, Hyperphosphorylation of microtubule-associated protein tau: a promising therapeutic target for Alzheimer disease, Curr. Med. Chem. 15 (23) (2008) 2321–2328.
[7] F.M. LaFerla, K.N. Green, S. Oddo, Intracellular amyloid-β in Alzheimer's disease, Nat. Rev. Neurosci. 8 (7) (2007) 499–509.
[8] E. Scarpini, P. Scheltens, H. Feldman, Treatment of Alzheimer's disease: current status and new perspectives, Lancet Neurol. 2 (9) (2003) 539–547.
[9] Q. Xie, H. Wang, Z. Xia, M. Lu, W. Zhang, X. Wang, W. Fu, Y. Tang, W. Sheng, W. Li, W. Zhou, X. Zhu, Z. Qiu, H. Chen, Bis-(-)-nor-meptazinols as novel nanomolar cholinesterase inhibitors with high inhibitory potency on amyloid-β aggregation, J. Med. Chem. 51 (7) (2008) 2027–2036.
[10] J.S. Lan, J.W. Hou, Y. Liu, Y. Ding, Y. Zhang, L. Li, T. Zhang, Design, synthesis and evaluation of novel cinnamic acid derivatives bearing N-benzyl pyridinium moiety as multifunctional cholinesterase inhibitors for Alzheimer's disease, J. Enzyme Inhib. Med. Chem. 32 (1) (2017) 776–788.
[11] D. Munoz-Torrero, Acetylcholinesterase inhibitors as disease-modifying therapies for Alzheimer's disease, Curr. Med. Chem. 15 (24) (2008).
[12] N. Herrmann, S.A. Chau, I. Kircanski, K.L. Lanctot, Current and emerging drug treatment options for Alzheimer's disease a systematic review, Drugs 71 (15) (2011) 2031–2065.
[13] D. Wilkinson, Y. Wirth, C. Goebel, Memantine in patients with moderate to severe Alzheimer's disease: meta-analyses using realistic definitions of response, Dement. Geriatr. Cogn. Disord. 37 (1–2) (2014) 71–85.
[14] L.D. Estrada, C. Soto, Disrupting β-amyloid aggregation for Alzheimer disease treatment, Curr. Top. Med. Chem. 7 (1) (2007) 115–126.
[15] R.L. Ildefonso, C.G.A. Laura, E.J.C. Maria, Protein misfolding and neurodegeneration, Rev. Mex. Neurocienc. 16 (1) (2015) 51–72.
[16] S. Paul, S. Planque, Y. Nishiyama, Beneficial catalytic immunity to Aβ peptide, Rejuvenat. Res. 13 (2–3) (2010) 179–187.
[17] M. Isabel Fernandez-Bachiller, C. Perez, G.C. Gonzalez-Munoz, S. Conde, M.G. Lopez, M. Villarroya, A.G. Garcia, M. Isabel Rodriguez-Franco, Novel tacrine-8-hydroxyquinoline hybrids as multifunctional agents for the treatment of Alzheimer's disease, with neuroprotective, cholinergic, antioxidant, and copper-complexing properties, J. Med. Chem. 53 (13) (2010) 4927–4937.
[18] A. Rauk, Why is the amyloid β peptide of Alzheimer's disease neurotoxic? Dalton Trans. 10 (2008) 1273–1282.
[19] G.J.M. Bruin, T. Faller, H. Wiegand, A. Schweitzer, H. Nick, J. Schneider, K.O. Boernsen, F. Waldmeier, Pharmacokinetics, distribution, metabolism, and excretion of deferasirox and its iron complex in rats, Drug Metab. Dispos. 36 (12) (2008) 2523–2538.
[20] J.L. Liu, Y.G. Fan, Z.S. Yang, Z.Y. Wang, C. Guo, Iron and Alzheimer's disease: from pathogenesis to therapeutic implications, Front. Neurosci. 12 (2018).
[21] G. Kamalinia, F. Khodagholi, F. Atyabi, M. Amini, F. Shaerzadeh, M. Sharifzadeh, R. Dinarvand, Enhanced brain delivery of deferasirox-lactoferrin conjugates for iron chelation therapy in neurodegenerative disorders: in Vitro and in Vivo studies, Mol. Pharmaceut. 10 (12) (2013) 4418–4431.
[22] S.Y. Li, N. Jiang, S.S. Xie, K.D.G. Wang, X.B. Wang, L.Y. Kong, Design, synthesis and evaluation of novel tacrine-rhein hybrids as multifunctional agents for the treatment of Alzheimer's disease, Org. Biomol. Chem. 12 (5) (2014) 801–814.
[23] P.B. Watkins, H.J. Zimmerman, M.J. Knapp, S.I. Gracon, K.W. Lewis, Hepatotoxic effects of tacrine administration in patients with Alzheimer's disease, JAMA 271 (13) (1994) 992–998.
[24] M.I. Fernandez-Bachiller, C. Perez, L. Monjas, J. Rademann, M.I. Rodriguez-Franco, New tacrine-4-Oxo-4H-chromene hybrids as multifunctional agents for the treatment of Alzheimer's disease, with cholinergic, antioxidant, and β-amyloid-reducing properties, J. Med. Chem. 55 (3) (2012) 1303–1317.
[25] X. Chen, K. Zenger, A. Lupp, B. Kling, J. Heilmann, C. Fleck, B. Kraus, M. Decker, Tacrine-silibinin codrug shows neuro- and hepato protective effects in vitro and pro-cognitive and hepatoprotective effects in vivo, J. Med. Chem. 55 (11) (2012) 5231–5242.
[26] K. Chand Rajeshwari, E. Candeias, S.M. Cardoso, S. Chaves, M. Amelia Santos, Tacrine-deferiprone hybrids as multi-target-directed metal chelators against Alzheimer's disease: a two-in-one drug, Metallomics 10 (10) (2018) 1460–1475.
[27] M.A. Santos, K. Chand, S. Chaves, Recent progress in multifunctional metal chelators as potential drugs for Alzheimer's disease, Coord. Chem. Rev. 327 (2016) 287–303.
[28] M.M. Khodaei, E. Nazari, Tf_2O-mediated direct and regiospecific para-acylation of phenols with carboxylic acids, Bull. Korean Chem. Soc. 32 (5) (2011) 1784–1786.
[29] Y.F. Han, C.P.L. Li, E. Chow, H. Wang, Y.P. Pang, P.R. Carlier, Dual-site binding of bivalent 4-aminopyridine- and 4-aminoquinoline-based AChE inhibitors: contribution of the hydrophobic alkylene tether to monomer and dimer affinities, Bioorg. Med. Chem. 7 (11) (1999) 2569–2575.
[30] W. F. Patton, J. Coleman, Y. Xiang, P. Pande, Z. Li, Autophagy and phospholipidosis pathway assays, Google Patents, 2016.
[31] M.G. Dickens, K.J. Franz, A prochelator activated by hydrogen peroxide prevents metal-induced amyloid β aggregation, ChemBioChem 11 (1) (2010) 59–62.
[32] U. Heinz, K. Hegetschweiler, P. Acklin, B. Faller, R. Lattmann, H.P. Schnebli, 4-3,5-Bis(2-hydroxyphenyl)-1,2,4-triazol-1-yl benzoic acid: a novel efficient and selective iron(III) complexing agent, Angewandte Chem.-Int. Ed. 38 (17) (1999) 2568–2570.
[33] E. Engvall, P. Perlmann, Enzyme-linked immunosorbent assay (ELISA) quantitative assay of immunoglobulin G, Immunochemistry 8 (9) (1971) 871–874.
[34] B.P. Doctor, T.C. Chapman, C.E. Christner, C.D. Deal, D.M.D.L. Hoz, M.K. Gentry, R.A. Ogert, R.S. Rush, K.K. Smyth, A.D. Wolfe, Complete amino acid sequence of fetal bovine serum acetylcholinesterase and its comparison in various regions with other cholinesterases, Febs Lett. 266 (1) (1990) 123–127.
[35] E.H. Rydberg, B. Brumshtein, H.M. Greenblatt, D.M. Wong, D. Shaya, L.D. Williams, P.R. Carlier, Y.P. Pang, I. Silman, J.L. Sussman, Complexes of alkylene-linked tacrine dimers with Torpedo californica acetylcholinesterase: Binding of bis(5)-tacrine produces a dramatic rearrangement in the active-site gorge, J. Med. Chem. 49 (18) (2006) 5491–5500.
[36] J.S. Lan, S.S. Xie, S.Y. Li, L.F. Pan, X.B. Wang, L.Y. Kong, Design, synthesis and evaluation of novel tacrine-(β-carboline) hybrids as multifunctional agents for the treatment of Alzheimer's disease, Bioorg. Med. Chem. 22 (21) (2014) 6089–6104.
[37] B.C. Magliaro, C.J. Saldanha, Clozapine protects PC-12 cells from death due to oxidative stress induced by hydrogen peroxide via a cell-type specific mechanism involving inhibition of extracellular signal-regulated kinase phosphorylation, Brain Res. 1283 (2009) 14–24.
[38] L.A. Greene, A.S. Tischler, Establishment of a noradrenergic clonal line of rat adrenal pheochromocytoma cells which respond to nerve growth factor, Proc. Natl. Acad. Sci. 73 (7) (1976) 2424–2428.
[39] M. Isabel Fernandez-Bachiller, C. Perez, N. Eugenia Campillo, J. Antonio Paez, G. Cristina Gonzalez-Munoz, P. Usan, E. Garcia-Palomero, M.G. Lopez, M. Villarroya, A.G. Garcia, A. Martinez, M. Isabel Rodriguez-Franco, Tacrine-melatonin hybrids as multifunctional agents for alzheimer's disease, with cholinergic antioxidant, and neuroprotective properties, Chemmedchem 4 (5) (2009) 828–841.
[40] M.S.J.N. Blois, Antioxidant determinations by the use of a stable free radical, Nature 181 (4617) (1958) 1199.
[41] C.A. Lipinski, F. Lombardo, B.W. Dominy, P.J. Feeney, Experimental and computational approaches to estimate solubility and permeability in drug discovery and development settings, Adv. Drug Deliv. Rev. 64 (2012) 4–17.
[42] S. Steinhauser, U. Heinz, J. Sander, K. Hegetschweiler, Complex formation of 2,6-bis-(2′-hydroxyphenyl)pyridine with Al-III, Fe-III and Cu-II, Zeitschrift Fur Anorganische Und Allgemeine Chemie 630 (12) (2004) 1829–1838.
[43] E. Engvall, K. Jonsson, P. Perlmann, Enzyme-linked immunosorbent assay. II. Quantitative assay of protein antigen, immunoglobulin G, by means of enzyme-labelled antigen and antibody-coated tubes, Biochimica et Biophysica Acta (BBA)-Protein, Structure 251 (3) (1971) 427–434.
[44] Glide, Version 6.7, Schrödinger, LLC, New York, NY, 2015.
[45] R.A. Friesner, J.L. Banks, R.B. Murphy, T.A. Halgren, J.J. Klicic, D.T. Mainz, M.P. Repasky, E.H. Knoll, M. Shelley, J.K. Perry, D.E. Shaw, P. Francis, P.S. Shenkin, Glide: A new approach for rapid, accurate docking and scoring. 1. Method and assessment of docking accuracy, J. Med. Chem. 47 (7) (2004) 1739–1749.